J Eng Math
DOI 10.1007/s10665-017-9934-6

On Boussinesq's problem for a cracked halfspace

A. P. S. Selvadurai

Received: 17 April 2017 / Accepted: 8 August 2017
© Springer Science+Business Media B.V. 2017

Abstract This paper examines the axisymmetric elastostatic problem that deals with the action of a concentrated normal force on the surface of an isotropic elastic halfspace containing a penny-shaped crack. The mathematical formulation of the elasticity problem should take into consideration the sense of action of the concentrated force. The paper presents the development of Fredholm integral equations of the second-kind that are associated with this category of problem and indicates the numerical technique that is adopted for their solution. The numerical results are presented for the stress intensity factors generated at the penny-shaped crack experiencing either opening or closure.

Keywords Boussinesq's problem · Fredholm integral equations of the second-kind · Mixed boundary value problems · Penny-shaped crack · Stress intensity factors

1 Introduction

The state of stress resulting from the action of a concentrated force directed normal to the surface of an isotropic elastic halfspace region is a celebrated problem in elasticity that was first examined by Boussinesq [1]. This classical result in elasticity is widely used in geomechanics and applied mechanics [2,3]. Boussinesq's approach for solving the problem of the loading of a halfspace by a concentrated normal force (Fig. 1) takes into account all the equations governing the classical theory of elasticity and the relevant boundary conditions and regularity conditions. Boussinesq [1] obtained the solution by referring to the results in potential theory that yield an *exact closed form solution* for the displacements and stresses within the halfspace region. An alternative approach to the development of the problem was presented by Selvadurai [4,5]. The classical study by Mindlin [6] represents the generalized result from which both Boussinesq's solution for the problem of the normal force acting at the surface of the halfspace and the solution by Kelvin [7] for the interior loading of an isotropic elastic halfspace by a concentrated force can be recovered as special cases (see also [8,9]).

William Scott Professor and James McGill Professor

A. P. S. Selvadurai (✉)
Department of Civil Engineering and Applied Mechanics, McGill University, Montreal H3A 0C3, QC, Canada
e-mail: patrick.selvadurai@mcgill.ca

Published online: 29 August 2017

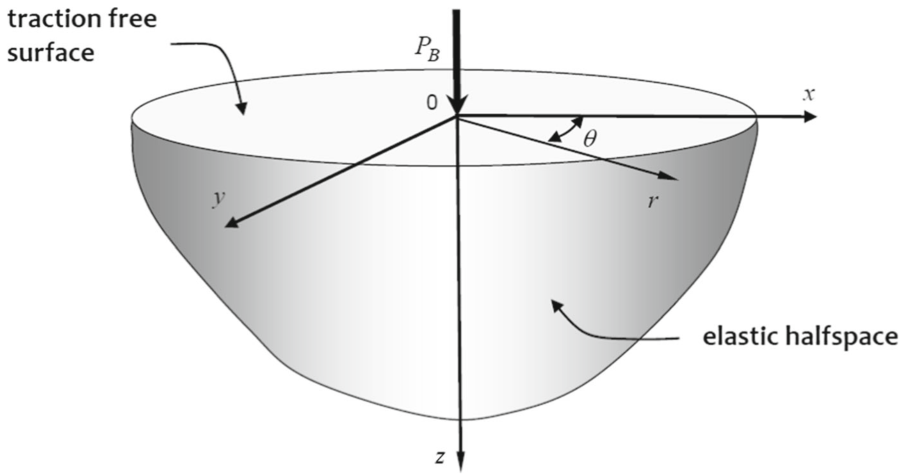

Fig. 1 Boussinesq's problem for a halfspace region

A result put forth by Fröhlich [10] examined the problem of the loading of the surface of a halfspace by a concentrated force, where the transfer of stresses within the halfspace is modified through the introduction of an exponent in the expressions obtained by Boussinesq. Selvadurai [11] showed that, while Fröhlich's result satisfies all the equations of equilibrium, the traction boundary conditions and regularity conditions, it violates the Beltrami–Michell equations of compatibility governing the strains. This leads to a *non-uniqueness* in evaluation of the displacement field, through the integration of the strain–displacement relations. The extension of the classical Boussinesq's problem to include anisotropy of the elastic material and elastic non-homogeneity is presented in several articles in elasticity theory and references to further work are given in [3].

The majority of problems dealing with the classical Boussinesq's problem relate to halfspace regions that are intact. The category of problems dealing with halfspace regions containing defects has received only limited attention. The defects could be either inclusions or cracks that are located within the halfspace region. The focus of this paper in particular is the interaction of the Boussinesq force and a penny-shaped crack located in a halfspace. The term "Penny-Shaped Crack" was first introduced by Sir Nevill Mott, who speculated that spherical gas bubbles in steel armour plates would become flattened during the rolling process to generate circular penny-shaped cracks [12].

Two classical papers on the penny-shaped crack problem, related to an isotropic elastic infinite space, were published by Sneddon [13], who examined the problem by employing the theory of dual integral equations and by Sack [14] who examined the problem by considering a spheroidal harmonics formulation where the penny-shaped crack was a special case of a flattened oblate spheroid. Since these seminal studies, the penny-shaped crack problem has been extended to include material anisotropy, material heterogeneity, functional grading of elastic properties, piezo-electro-elasticity, bi-material regions, etc. Complete coverage of all the articles related to penny-shaped cracks is, however, beyond the scope of this paper.

Studies dealing with cracks in halfspace regions are of special relevance to the problems examined in this paper, and these will be discussed. Furthermore, if a mathematical analysis of the influence of a defect is contemplated, the geometry of the resulting problem must be amenable to a convenient mathematical formulation that is employed in the solution of problems in elasticity theory. The term "inclusion" is intended to describe a region that has elasticity properties different from the exterior elastic medium. The inclusion is generally regarded as a rigid defect and when the inclusion detaches from the surrounding elastic medium, the detached surface is regarded as a crack. When the inclusion is a plane disc, which is bonded to the surrounding elastic medium of the halfspace, the problem can be formulated using to integral equation techniques employed in classical elasticity theory [15,16]. The axisymmetric problem of the axial loading of a rigid disc anchor embedded in an incompressible elastic halfspace region was examined by Hunter and Gamblen [17], and the base of the disc anchor was considered to

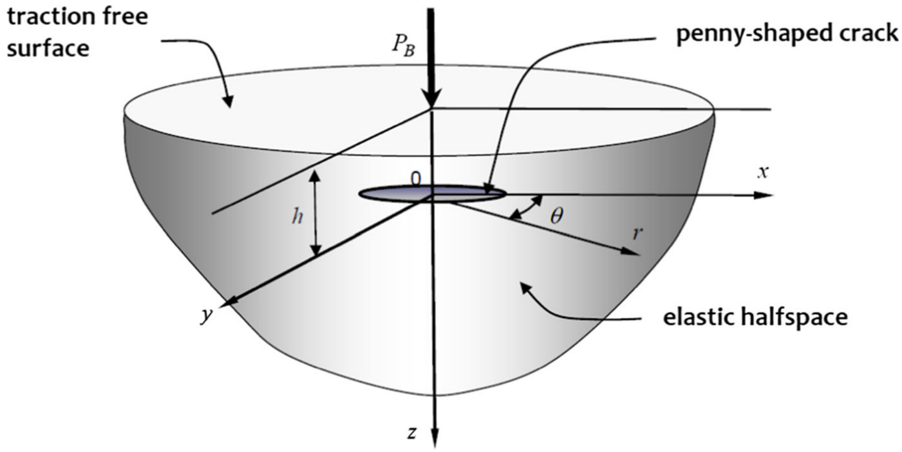

Fig. 2 Loading of halfspace containing a penny-shaped crack by a Boussinesq force

be either completely adhering or detached. The analysis provided estimates for the elastic stiffness of the rigid disc anchor, which has applications in the area of geomechanics of ground anchors [18]. The analysis by Keer [19] examines the problem of the axial loading of a rigid disc inclusion that is bonded to a single face of a penny-shaped crack. The study also examines the nature of the oscillatory form of the singularity that can be present at the boundary of the penny-shaped crack that is reinforced by a rigid inclusion on one of its faces. Boussinesq surface loading of a halfspace containing a bonded rigid disc inclusion is presented in [20], while Boussinesq force loading of *halfspaces*, containing bonded and partially bonded disc inclusions are presented in [21,22]. The problem examined in [22] considers the axisymmetric problem of a halfspace containing a penny-shaped crack but subjected to opening by a rigid circular indentor bonded to the surface of the halfspace. This problem also results in a mixed boundary value problem for the indentor but generates both Mode I and Mode II stress intensity factors at the crack tip.

The problem of a penny-shaped crack located within a halfspace region has also been examined by a number of researchers; Smith and Alavi [23] examined the problem of a halfspace containing a penny-shaped crack the plane of which is normal to the traction-free surface of a halfspace. The problem of a pressurized crack in a halfspace was examined by Srivastava and Singh [24], and a more general problem of a penny-shaped crack situated in a layer bonded to dissimilar halfspace regions was examined by Erdogan and Arin [25]. Extensive accounts of the axisymmetric problem of a penny-shaped crack located in an isotropic elastic halfspace region are given by Sneddon and Lowengrub [26], Kassir and Sih [27], Cherepanov [28] and Broberg [29]. In a majority of these cases, the penny-shaped crack is subjected to internal pressurization, which constitutes a problem of interest to the development of gas pressures in defects located near the surface of an elastic solid.

The problem involving the action of a Boussinesq-type concentrated load at the surface of a halfspace region containing a penny-shaped crack is relevant to the study of contact mechanics of halfspace regions with a buried defect. In this paper, we examine the axisymmetric problem of the action of a Boussinesq force on the surface of a halfspace containing a penny-shaped crack (Fig. 2). Unlike the case involving the direct loading of the surfaces of the penny-shaped crack by surface tractions, the action of the surface Boussinesq force can influence the boundary conditions that can be specified on the faces of the crack. When the Boussinesq force is directed away from the surface of the halfspace, traction-free boundary conditions are applicable to the faces of the crack. When the Boussinesq force is directed towards the interior of the halfspace, the surfaces of the penny-shaped crack can be subjected to mixed boundary conditions that could also involve unilateral contact. This paper examines the mathematical developments of the boundary value problems, and these mathematical developments are used to determine the stress intensity factors at the tip of the penny-shaped crack.

2 Governing equations

We consider the state of axial symmetry in the associated elasticity problem defined by the state of deformation:

$$\mathbf{u} = (u_r(r,z), 0, u_r(r,z)), \tag{1}$$

where $u_r(r,z)$ and $u_z(r,z)$ are the displacement components referred to the axisymmetric system of coordinates (r,z). The strain tensor $\boldsymbol{\varepsilon}$ is given by

$$\boldsymbol{\varepsilon} = \begin{pmatrix} \frac{\partial u_r}{\partial r} & 0 & \frac{1}{2}\left(\frac{\partial u_r}{\partial z} + \frac{\partial u_z}{\partial r}\right) \\ 0 & \frac{u_r}{r} & 0 \\ \frac{1}{2}\left(\frac{\partial u_r}{\partial z} + \frac{\partial u_z}{\partial r}\right) & 0 & \frac{\partial u_z}{\partial z} \end{pmatrix}. \tag{2}$$

The state of stress in the elastic region is defined by the stress tensor

$$\boldsymbol{\sigma} = \begin{pmatrix} \sigma_{rr} & 0 & \sigma_{rz} \\ 0 & \sigma_{\theta\theta} & 0 \\ \sigma_{rz} & 0 & \sigma_{zz} \end{pmatrix}. \tag{3}$$

The stress–strain relationship for the elastic material corresponds to Hooke's law:

$$\boldsymbol{\sigma} = \lambda e\,\mathbf{I} + 2\mu\boldsymbol{\varepsilon}, \tag{4}$$

where $e = \mathrm{tr}\,\varepsilon$ and λ and μ are Lamé's constants, $\mathbf{I}$ is the identity tensor and, in the absence of body forces, the equations of equilibrium reduce to

$$\nabla \cdot \boldsymbol{\sigma} = \mathbf{0}, \tag{5}$$

and $\nabla\cdot$ is the divergence operator. The solution of the equations of elasticity governing the axisymmetric problem can be approached in a variety of ways, and these are described in several texts in classical elasticity theory.

3 Boussinesq's problem for a cracked elastic halfspace

We consider the axisymmetric problem related to an isotropic elastic halfspace containing a penny-shaped crack loaded by a concentrated Boussinesq force, which preserves axial symmetry. In this situation, the mixed boundary value problem related to the crack has to take into account the sense of application of the Boussinesq force. We consider the elastic domain to be composed of a layer region (superscript$^{(1)}$) occupying the domain $r \in (0,\infty)$, $z \in (-h, 0)$ and a halfspace region (superscript$^{(2)}$) occupying the domain $r \in (0,\infty)$, $z \in (0,\infty)$ (Fig. 2). We first consider Boussinesq's problem of an intact halfspace with the coordinate configuration corresponding to the identified layer region$^{(1)}$ and the halfspace region$^{(2)}$ (Fig. 3), which is subjected to a concentrated force acting along the positive z-direction. The stresses acting on the plane $z = 0$ can be written as [2,5,33]

$$\sigma_{zz}(r,0) = -\frac{3P}{2\pi}\frac{h^3}{(r^2+h^2)^{5/2}} = f(r), \tag{6}$$

$$\sigma_{rz}(r,0) = -\frac{3P}{2\pi}\frac{rh^2}{(r^2+h^2)^{5/2}} = g(r). \tag{7}$$

The formulation of the axisymmetric mixed boundary value problems in classical elasticity that will be presented in this paper can be approached in a variety of ways; here, we adopt the solution procedure involving two harmonic functions $\varphi(r, z)$and $\psi(r, z)$ (see, e.g. [30–32]), which satisfy

$$\nabla^2\varphi(r, z) = 0; \quad \nabla^2\psi(r, z) = 0, \tag{8}$$

where ∇^2 is the axisymmetric form of Laplace's operator referred to the cylindrical polar coordinate system, given by

$$\nabla^2 = \frac{\partial^2}{\partial r^2} + \frac{1}{r}\frac{\partial}{\partial r} + \frac{\partial^2}{\partial z^2}. \tag{9}$$

The displacements and stress components derived from these harmonic functions can be expressed in the form:

$$u_r = \frac{\partial\varphi}{\partial r} - z\frac{\partial\psi}{\partial r}, \tag{10}$$

$$u_z = (3-4\nu)\psi + \frac{\partial\varphi}{\partial z} - z\frac{\partial\psi}{\partial z} \tag{11}$$

and

$$\sigma_{rr} = 2\mu\left(\frac{\partial^2\varphi}{\partial r^2} + 2\nu\frac{\partial\psi}{\partial z} - z\frac{\partial^2\psi}{\partial r^2}\right), \tag{12}$$

$$\sigma_{\theta\theta} = 2\mu\left(\frac{1}{r}\frac{\partial\varphi}{\partial r} + 2\nu\frac{\partial\psi}{\partial z} - \frac{z}{r}\frac{\partial\psi}{\partial r}\right), \tag{13}$$

$$\sigma_{zz} = 2\mu\left(2(1-\nu)\frac{\partial\psi}{\partial z} + \frac{\partial^2\varphi}{\partial z^2} - z\frac{\partial^2\psi}{\partial z^2}\right), \tag{14}$$

$$\sigma_{rz} = 2\mu\left((1-2\nu)\frac{\partial\psi}{\partial r} + \frac{\partial^2\varphi}{\partial r\partial z} - z\frac{\partial^2\psi}{\partial r\partial z}\right). \tag{15}$$

3.1 The closed crack problem

We consider the problem where the action of the compressive Boussinesq force maintains the penny-shaped crack in a closed condition over its entire region (Fig. 3). This assumption is applicable if the penny-shaped crack is located remote from the surface of the halfspace, which can ensure the closure of the crack under the action of the compressive Boussinesq force. In situations where the penny-shaped crack is located close to the surface of the halfspace, it is plausible that the action of the compressive force will induce closure over a part of the crack and opening over the exterior region due to the flexural action of the elastic plate-like zone above the penny-shaped crack (Fig. 4). This will result in a unilateral contact problem of the Signorini-type, where the radius of the zone of contact needs to be determined by considering a Barenblatt-type constraint requiring the vanishing of the contact stress at the point of separation. In this study, we shall assume that there is complete closure of the penny-shaped crack due to the action of the compressive Boussinesq force.

The complete solution to the problem of a penny-shaped crack that maintains frictionless contact over its entire surface can be obtained by *combining* the solution to (i) Boussinesq's problem referred to an intact halfspace with (ii) a corrective solution that will satisfy the following set of boundary and continuity conditions:

$$\sigma_{zz}^{(1)}(r, -h) = 0; \; \sigma_{rz}^{(1)}(r, -h) = 0; \; r > 0, \tag{16}$$

$$\sigma_{rz}^{(1)}(r, 0) = -g(r); \; \sigma_{rz}^{(2)}(r, 0) = -g(r); \; 0 < r < a, \tag{17}$$

$$u_z^{(1)}(r, 0) = u_z^{(2)}(r, 0); \; r \geq 0, \tag{18}$$

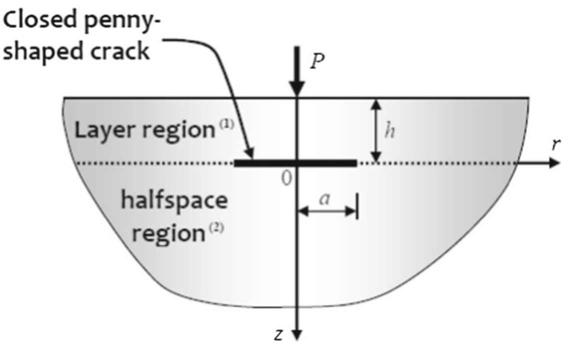

Fig. 3 The closed penny-shaped crack problem

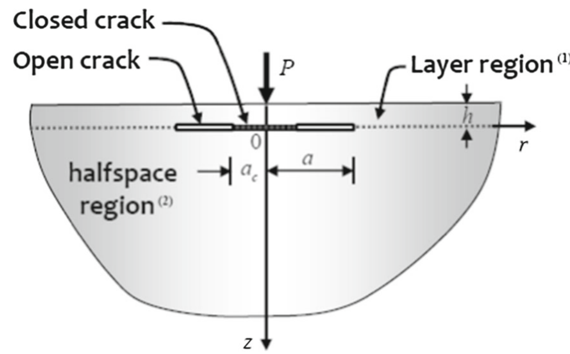

Fig. 4 The partially closed penny-shaped crack problem

$$u_r^{(1)}(r,0) = u_r^{(2)}(r,0);\ \ a \le r < \infty, \tag{19}$$

$$\sigma_{rz}^{(1)}(r,0) = \sigma_{rz}^{(2)}(r,0);\ \ a \le r < \infty, \tag{20}$$

The combination of solutions will satisfy the traction boundary conditions on the surface of the halfspace corresponding to the Boussinesq force, render the faces of the penny-shaped crack free of shear tractions and satisfy the regularity conditions applicable to the decay of stresses and displacements in the halfspace region (i.e. the displacement field should exhibit a decay $\mathrm{O}(R^{-1})$ and the stress field should exhibit a decay $\mathrm{O}(R^{-2})$, where $R = (r^2 + z^2)^{1/2}$).

For the solution of the mixed boundary value problem defined by (16)–(20), we use the Hankel integral transform-based general solutions of $\varphi(r,z)$and $\psi(r,z)$ applicable to both domains of finite and infinite extents in z. We have

$$\varphi(r,z) = \int_0^\infty \left[A_1(\xi)\mathrm{e}^{\xi z} + A_2(\xi)\mathrm{e}^{-\xi z} + A_3(\xi)z\mathrm{e}^{\xi z} + A_4(\xi)z\mathrm{e}^{-\xi z}\right]\ J_0(\xi r)\mathrm{d}\xi, \tag{21}$$

$$\psi(r,z) = \int_0^\infty \left[B_1(\xi)\mathrm{e}^{\xi z} + B_2(\xi)\mathrm{e}^{-\xi z} + B_3(\xi)z\mathrm{e}^{\xi z} + B_4(\xi)z\mathrm{e}^{-\xi z}\right]\ J_0(\xi r)\mathrm{d}\xi, \tag{22}$$

where $A_n(\xi)$ and $B_n(\xi)$ are arbitrary functions that need to be determined by satisfying the boundary conditions and regularity conditions applicable to the closed crack problem. Many of the arbitrary functions can be eliminated through the application of the boundary and continuity conditions at the plane $z = 0$, containing the closed penny-shaped crack. For example, the relevant expressions for the displacement components and the stress components applicable to the halfspace region$^{(2)}$can be written as

$$u_r^{(2)}(r,z) = \int_0^\infty [A(s) + szB(s)]\ \mathrm{e}^{-sz} J_1(sr)\mathrm{d}s, \tag{23}$$

$$u_z^{(2)}(r,z) = \int_0^\infty [A(s) + (3-4\nu)B(s) + szB(s)]\ \mathrm{e}^{-sz} J_0(sr)\mathrm{d}s, \tag{24}$$

$$\sigma_{zz}^{(2)}(r,z) = -2\mu \int_0^\infty s\,[A(s) + 2(1-\nu)B(s) + szB(s)]\ \mathrm{e}^{-sz} J_0(sr)\mathrm{d}s, \tag{25}$$

$$\sigma_{rz}^{(2)}(r,z) = -2\mu \int_0^\infty s\,[A(s) + (1-2\nu)B(s) + szB(s)]\ \mathrm{e}^{-sz} J_1(sr)\mathrm{d}s. \tag{26}$$

The relevant displacement and stress components applicable to the layer region$^{(1)}$ can be written as

$$u_r^{(1)}(r,z) = \int_0^\infty \left\{ \begin{array}{l} [s(z+h)C(s) - 2(1-\nu)D(s)]\ \cosh[s(z+h)] \\ +[(1-2\nu)C(s) - s(z+h)D(s)]\sinh[s(z+h)] \end{array} \right\} \frac{J_1(rs)}{\sinh(sh)}\mathrm{d}s, \tag{27}$$

$$u_z^{(1)}(r,z) = \int_0^\infty \left\{ \begin{array}{l} [2(1-\nu)C(s)+s(z+h)D(s)]\ \cosh[s(z+h)] \\ -[s(z+h)C(s)+(1-2\nu)D(s)]\sinh[s(z+h)] \end{array} \right\} \frac{J_0(rs)}{\sinh(sh)}\mathrm{d}s, \tag{28}$$

$$\sigma_{zz}^{(1)}(r,z) = 2\mu \int_0^\infty \left\{ \begin{array}{l} [C(s)+s(z+h)D(s)]\ \sinh[s(z+h)] \\ -s(z+h)C(s)\cosh[s(z+h)] \end{array} \right\} \frac{sJ_0(rs)}{\sinh(sh)}\mathrm{d}s, \tag{29}$$

$$\sigma_{rz}^{(1)}(r,z) = -2\mu \int_0^\infty \left\{ \begin{array}{l} [D(s)-s(z+h)C(s)]\ \sinh[s(z+h)] \\ +s(z+h)D(s)\cosh[s(z+h)] \end{array} \right\} \frac{sJ_1(rs)}{\sinh(sh)}\mathrm{d}s. \tag{30}$$

Avoiding details, it can be shown that by using the final expression for the relevant displacement and stress components in the layer$^{(1)}$ and halfspace$^{(2)}$ regions, we can effectively reduce the boundary and continuity conditions (16)–(20) to the following set of dual integral equations:

$$\int_0^\infty sF_1(s)K(sh)J_1(sr)\mathrm{d}s = -\frac{g(r)}{2\mu}; \quad 0 \le r \le a, \tag{31}$$

$$\int_0^\infty F_1(s)J_1(sr)\mathrm{d}s = 0; \quad a < r < \infty, \tag{32}$$

where

$$F_1(s) = D(s)\left[\frac{2-sh+sh\coth(sh)}{(1-sh)}\right], \tag{33}$$

$$K(sh) = \frac{(1-sh)[1+sh\coth(sh)]+(sh)^2}{\{2-sh+sh\coth(sh)\}}. \tag{34}$$

The reduction of the dual system (31) and (32) to a single Fredholm integral equation of the second-kind is given by Sneddon [15,16] and Sneddon and Lowengrub [26]. Introducing the representation,

$$F_1(s) = -\frac{\sqrt{s}}{\mu}\int_0^a \sqrt{t}\ \Psi(t)\ J_{3/2}(st)\ \mathrm{d}t \tag{35}$$

with the requirement that

$$\lim_{t\to 0}\,[t\ \Psi(t)] = 0 \tag{36}$$

the dual system can be reduced to a single Fredholm integral equation of the second-kind

$$\Psi(t) + \int_0^a \Psi(s)L(s,t)\ \mathrm{d}s = \frac{2}{t\sqrt{2\pi}}\int_0^t \frac{r^2 g(r)}{\sqrt{t^2-r^2}}\mathrm{d}r, \tag{37}$$

where the Kernel function $L\ (s,t)$ is given by

$$L(s,t) = 2\sqrt{st}\int_0^\infty \eta\left(K(\eta h) - \frac{1}{2}\right) J_{3/2}(\eta t)J_{3/2}(\eta s)\ \mathrm{d}\eta. \tag{38}$$

The numerical solution of the Fredholm integral equation of the second-kind (37) can be used to evaluate displacement and stress fields within the halfspace containing the penny-shaped crack. When dealing with cracks within an elastic body, a result of particular interest to fracture mechanics and the extension of the crack relates to the stress intensity factor at the crack tip. At the boundary of the closed penny-shaped crack, the Mode II stress intensity factor is given by

$$\mathrm{K_{II}} = \operatorname*{Lim}_{r \to a} \left[\sqrt{2(r-a)} \sigma_{rz}^{(1)}(r, 0) \right], \tag{39}$$

which can be expressed in the form

$$\mathrm{K_{II}} = \sqrt{\frac{2}{\pi}} \frac{\Psi(a)}{\sqrt{a}}. \tag{40}$$

3.1.1 Numerical solution of the governing integral equation

To the author's knowledge, the governing Fredholm integral equation of the second-kind (37) has no known exact solution and recourse must be made to numerical methods for its solution. Extensive accounts of procedures that can be adopted for the solution of Fredholm integral equations are given in [34–38].

Using the result (7), the integral equation can be reduced to the form

$$\Psi(t) + \int_0^a \Psi(s) L(s, t)\, \mathrm{d}s = \frac{4P}{(2\pi)^{3/2}} \frac{ht^2}{(h^2+t^2)^2}; \quad 0 < t < a, \tag{41}$$

and the kernel function can be expressed as

$$L(s, t) = \sqrt{st} \int_0^\infty \frac{\eta h(1-2\eta h)\mathrm{e}^{-2\eta h}}{\left[1-(1-\eta h)\mathrm{e}^{-2\eta h}\right]} \eta J_{3/2}(\eta t) J_{3/2}(\eta s)\, \mathrm{d}\eta. \tag{42}$$

To solve the integral equation (41) numerically, we discretize the interval $(0, a]$ into N segments with

$$\begin{aligned} s_i &= (i-1)\frac{a}{N}; \quad (i = 1, 2, 3, \ldots, N+1), \\ t_i &= \frac{1}{2}(s_i + s_{i+1}); \quad (i = 1, 2, 3, \ldots, N). \end{aligned} \tag{43}$$

The discretized equivalent of the Fredholm integral equation (41) can be expressed in the form

$$\Psi(t_i) + \frac{a}{N} \sum_{j=1}^{N} \Psi(t_i) L(t_j, t_i) = \frac{4P}{(2\pi)^{3/2}} \frac{ht_i^2}{(h^2+t_i^2)^2}; \quad i = 1, 2, \ldots, N. \tag{44}$$

The accuracy of the collocation technique has been verified through comparisons with analytical results, and the kernel function can be accurately evaluated using a Gaussian quadrature technique. Upon applying the solution of the set of equations (44) for the values of $\Psi(t)$ at the discrete locations t_N, the normalized Mode II stress intensity factor can be expressed in the form:

$$\bar{\mathrm{K}}_{\mathrm{II}}^a = \frac{\mathrm{K}_{\mathrm{II}}^a}{P/a^{3/2}} = \sqrt{\frac{2}{\pi}} \frac{a}{P} \Psi(t_N). \tag{45}$$

It should be noted that only the corrective solution will contain the singular fields at the location corresponding to the boundary of the penny-shaped crack, which can be used to estimate the Mode II stress intensity factor at the crack tip.

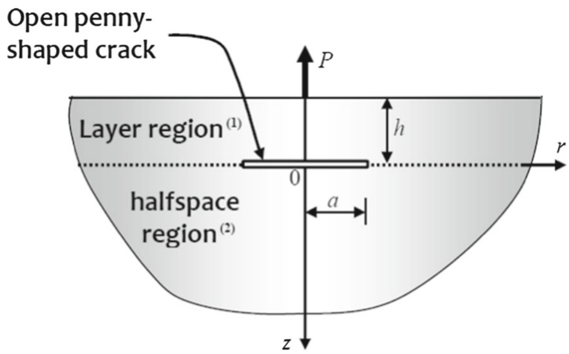

Fig. 5 The open penny-shaped crack problem

3.2 The open crack problem

We now consider the axisymmetric problem of the loading of a halfspace containing a penny-shaped crack by a Boussinesq force that is tensile in nature (Fig. 5). In this instance, the application of tensile loads will maintain the crack in an open state, and the faces of the crack will be traction free.

We examine the additive problem related to the open crack, which is defined by the following boundary value problem, referred to the layer (superscript$^{(1)}$) and halfspace (superscript$^{(2)}$) domains:

$$\sigma_{zz}^{(1)}(r,-h)=0;\ \sigma_{rz}^{(1)}(r,-h)=0;\ r>0, \tag{46}$$

$$u_z^{(1)}(r,0)=u_z^{(2)}(r,0);\ a\le r<\infty, \tag{47}$$

$$u_r^{(1)}(r,0)=u_r^{(2)}(r,0);\ a\le r<\infty, \tag{48}$$

$$\sigma_{zz}^{(1)}(r,0)=\ \sigma_{zz}^{(2)}(r,0)=-f(r);\ 0\le r<a, \tag{49}$$

$$\sigma_{rz}^{(1)}(r,0)=\ \sigma_{rz}^{(2)}(r,0)=-g(r);\ 0\le r<a, \tag{50}$$

$$\sigma_{zz}^{(1)}(r,0)=\ \sigma_{zz}^{(2)}(r,0);\quad a<r<\infty, \tag{51}$$

$$\sigma_{rz}^{(1)}(r,0)=\ \sigma_{zz}^{(2)}(r,0);\quad a<r<\infty. \tag{52}$$

The displacement and stress fields derived from the solution of the boundary value problem defined by (46) to (52) together with the Boussinesq solution for the intact halfspace should give rise to displacement and stress fields that exhibit spatial decays of the order $\mathrm{O}(R^{-1})$ and $\mathrm{O}(R^{-2})$, respectively, where $R=(r^2+z^2)^{1/2}$. The solutions (21) and (22) presented previously, for $\varphi(r,z)$and $\psi(r,z)$, respectively, can be used to formulate the governing integral equations.

The integral equations governing the open crack problem can be formulated using the expressions (23) to (30) for the relevant displacement and stress components in the layer and halfspace regions and the boundary and continuity conditions governing the problem are given by

$$\frac{1}{2}\int_0^\infty sM(s)J_0(rs)\mathrm{d}s+\int_0^\infty\left\{\begin{array}{l}L(s)\left[\alpha\left\{1-sh\coth(sh)\right\}+sh\gamma\right]\\+M(s)\left[\beta\left\{1-sh\coth(sh)\right\}+\delta sh-\frac{1}{2}\right]\end{array}\right\}sJ_0(rs)\mathrm{d}s=-\frac{f(r)}{2\mu};\quad 0<r<a, \tag{53}$$

$$-\frac{1}{2}\int_0^\infty sL(s)J_1(rs)\mathrm{d}s+\int_0^\infty\left\{\begin{array}{l}L(s)\left[\gamma\left\{1+sh\coth(sh)\right\}-sh\alpha+\frac{1}{2}\right]\\+M(s)\left[\delta\left\{1+sh\coth(sh)\right\}-\beta sh\right]\end{array}\right\}sJ_1(rs)\mathrm{d}s=\frac{g(r)}{2\mu};\quad 0<r<a, \tag{54}$$

$$\int_0^\infty L(s)J_1(rs)\mathrm{d}s=0;\quad a<r<\infty, \tag{55}$$

$$\int_0^\infty M(s) J_0(rs) \mathrm{d}s = 0; \quad a < r < \infty, \tag{56}$$

where

$$L(s) = [shC(s) - D(s)\{1 + sh\}]\{1 + \coth(sh)\}, \tag{57}$$

$$M(s) = [(1 - sh)C(s) - D(s)sh]\{1 + \coth(sh)\}. \tag{58}$$

We can express the functions $C(s)$ and $D(s)$ in the forms

$$C(s) = \alpha L(s) + \beta M(s); \quad D(s) = \gamma L(s) + \delta M(s) \tag{59}$$

and

$$\alpha = \frac{1 + \gamma\{1 + sh\}}{sh}; \quad \beta = \frac{\delta\{1 + sh\}}{sh},$$
$$\gamma = -\frac{\{1 - sh\}}{[1 + \coth(sh)]}; \quad \delta = \frac{sh}{[1 + \coth(sh)]}. \tag{60}$$

The coupled system of integral equations (53) to (56) can be solved using the procedures given by Copson [39]. We introduce finite transforms such that

$$L(s) = \sqrt{s}\int_0^a \Psi(t) J_{3/2}(st)\,\mathrm{d}t = \frac{1}{s}\left(\frac{2}{\pi}\right)^{1/2}\left[-\frac{\Psi(a)}{\sqrt{a}}\sin(as) + \int_0^a \frac{\sin(st)}{t}\left\{\sqrt{t}\Psi(t)\right\}'\mathrm{d}t\right], \tag{61}$$

$$M(s) = \int_0^a \Phi(t)\sin(st)\,\mathrm{d}t = \frac{1}{s}\left[-\Phi(a)\cos(as) + \int_0^a \Phi'(t)\cos(st)\mathrm{d}t\right], \tag{62}$$

where the prime denotes differentiation with respect to the argument.

The functions $\Phi(r)$ and $\Psi(r)$ in (61) and (62) must satisfy the conditions

$$\operatorname*{Lim}_{t\to 0}\left[t^{1/2}\Psi(t)\right] = 0; \quad \operatorname*{Lim}_{t\to 0}[\Phi(t)] = 0. \tag{63}$$

Equations (61) and (62) satisfy Eqs. (55) and (56). Substituting the representations (61) and (62) in (53) and (54), we obtain

$$\int_0^r \frac{\Phi'(t)\mathrm{d}t}{\left(r^2 - t^2\right)^{1/2}} = -\frac{f(r)}{\mu} - 2\int_0^\infty \left\{\begin{array}{l} L(s)\left[\alpha\{1 - sh\coth(sh)\} + \gamma sh\right] \\ +M(s)\left[\beta\{1 - sh\coth(sh)\} + \delta sh - \frac{1}{2}\right]\end{array}\right\} sJ_0(sr)\mathrm{d}s; \; 0 < r < a, \tag{64}$$

$$\sqrt{\frac{2}{\pi}}\int_0^r \frac{\left[\sqrt{t}\Psi(t)\right]'\mathrm{d}t}{\left(r^2 - t^2\right)^{1/2}} = -\frac{rg(s)}{\mu} + 2r\int_0^\infty \left\{\begin{array}{l} L(s)\left[\gamma\{1 + sh\coth(sh)\} - \alpha sh + \frac{1}{2}\right] \\ +M(s)\left[\delta\{1 + sh\coth(sh)\} - \beta sh\right]\end{array}\right\} sJ_1(rs)\mathrm{d}s; \; 0 < r < a. \tag{65}$$

With the aid of the results

$$\int_0^t \frac{rJ_0(rs)\mathrm{d}r}{(t^2 - r^2)^{1/2}} = \frac{\sin(ts)}{s}, \tag{66}$$

$$\int_0^t \frac{r^2 J_1(rs)\mathrm{d}r}{(t^2 - r^2)^{1/2}} = \left(\frac{\pi}{2s}\right)^{1/2} t^{3/2} J_{3/2}(st), \tag{67}$$

Eqs. (64) and (65) can be inverted to give the following pair of coupled integral equations for the unknown functions $\Phi(t)$and $\Psi(t)$:

$$\Phi(t) = -\frac{2}{\pi\mu}\int_0^t \frac{rf(r)\,\mathrm{d}r}{\sqrt{t^2-r^2}} + \frac{2}{\pi}\int_0^a [\Psi(r)R(t,r) + \Phi(r)S(t,r)]\mathrm{d}r;\quad 0 < t < a, \tag{68}$$

$$\Psi(t) = -\frac{1}{\mu}\left(\frac{2}{\pi t}\right)^{1/2}\int_0^t \frac{r^2 g(r)\,\mathrm{d}r}{\sqrt{t^2-r^2}} + \int_0^a [\Psi(r)T(t,r) + \Phi(r)U(t,r)]\mathrm{d}r;\quad 0 < t < a, \tag{69}$$

where

$$R(r,t) = -2\int_0^\infty \sqrt{s}\sin(st)J_{3/2}(sr)[\alpha\{1 - sh\coth(sh)\} + \gamma sh]\mathrm{d}s, \tag{70}$$

$$S(r,t) = -2\int_0^\infty \sin(st)\sin(sr)\left\{\beta[1 - sh\coth(sh)] + \delta sh - \frac{1}{2}\right\}\mathrm{d}s, \tag{71}$$

$$T(r,t) = 2t\int_0^\infty s\left[\gamma\{1 + sh\coth(sh)\} - \alpha sh + \frac{1}{2}\right]J_{3/2}(st)J_{3/2}(sr)\mathrm{d}s, \tag{72}$$

$$U(r,t) = 2t\int_0^\infty \sqrt{s}\sin(sr)J_{3/2}(sr)[\delta\{1 + sh\coth(sh)\} - \beta sh]\,\mathrm{d}s. \tag{73}$$

It may be noted that as $h \to \infty$, the functions $f,\ g,\ R,\ S,\ T$and U all reduce to zero, and the interaction between the Boussinesq force and the penny-shaped crack is absent.

3.2.1 Numerical solution of the governing coupled integral equations

Using the expressions for $f(r)$ and $g(r)$, the coupled system of integral equations for $\Psi(t)$ and $\Phi(t)$ can be written as

$$\Phi(t) - \frac{2}{\pi}\int_0^a \Phi(r)S(r,t)\mathrm{d}r - \frac{2}{\pi}\int_0^a \Psi(r)R(r,t)\mathrm{d}r = -\frac{Pt(3h^2+t^2)}{\pi^2\mu(t^2+h^2)^2};\quad 0 < t < a, \tag{74}$$

$$\Psi(t) - \int_0^a \Phi(r)S_1(r,t)\mathrm{d}r - \int_0^a \Psi(r)R_1(r,t)\mathrm{d}r = -\sqrt{\frac{2}{\pi}}\frac{Pht^{5/2}}{\pi\mu(t^2+h^2)^2};\quad 0 < t < a. \tag{75}$$

For the solution of the coupled system of integral equations (73) and (74), we employ a discretization procedure where the interval $(0, a]$ is divided into N segments with

$$r_i = (i-1)\frac{a}{N};\quad i = 1, 2, \ldots, N+1, \tag{76}$$

and the collocation points are given by

$$t_i = \frac{1}{2}(r_i + r_{i+1});\quad i = 1, 2, \ldots, N. \tag{77}$$

The system of coupled integral equations (74) and (75) can be reduced to a matrix equation of the form:

$$[\mathbf{A}_{ij}]\{\boldsymbol{\Lambda}_j\} = \{\mathbf{B}_i\}, \tag{78}$$

where $i, j = 1, 2, \ldots, 2N$. The coefficients $\mathbf{A}_{ij}$ are given by

$$A_{2l-1,2m-1} = \delta_{lm} - \frac{2}{\pi}S(t_l,t_m)\frac{a}{N};\quad A_{2l-1,2m} = -\frac{2}{\pi}R(t_l,t_m)\frac{a}{N},$$

$$A_{2l,2m-1} = -S_1(t_l,t_m)\frac{a}{N};\quad A_{2l,2m} = \delta_{lm} - \frac{2}{\pi}R_1(t_l,t_m)\frac{a}{N}s, \tag{79}$$

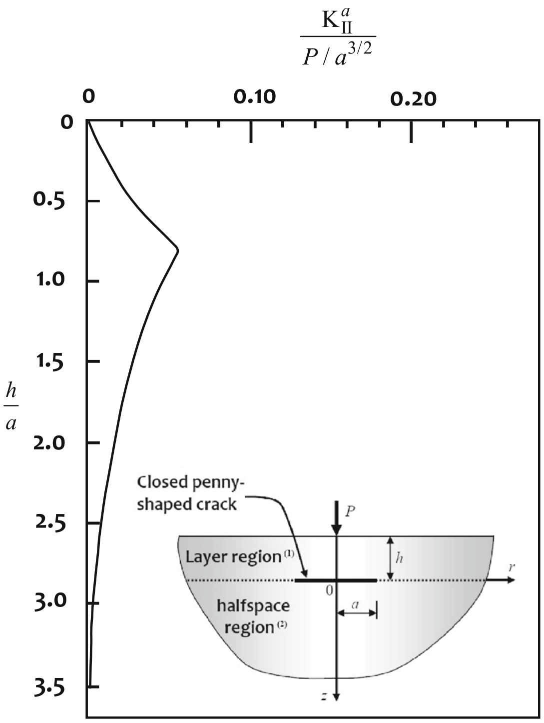

Fig. 6 Mode II stress intensity factor for the closed penny-shaped crack shown in Fig. 3

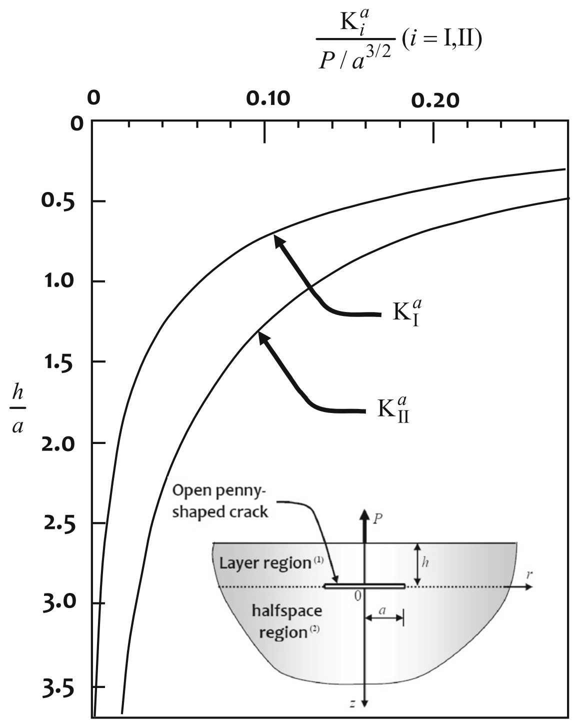

Fig. 7 Mode I and Mode II stress intensity factors for the open penny-shaped crack shown in Fig. 5

where δ_{lm} is Kronecker's delta function and $l, m = 1, 2, \ldots, N$. In (79), the Kernel functions at (t_l, t_m) can be evaluated to within an accuracy of 10^{-5}using a Gaussian quadrature technique. The matrix $\left[\mathbf{A}_{ij}\right]$ is fully populated and positive definite. The inversion of (78) for $N = 10$ can be accomplished using a Gaussian elimination technique. Again, the accuracy of the numerical scheme for $N = 10$ has also been verified in previous studies dealing with both crack and inclusion problems for which exact closed-form results were available. Increase in the vector on the right-hand side of (78) is given by

$$B_{2l-1} = \frac{Pt_l(3h^2 + t_l^2)}{\pi^2\mu(t_l^2 + h^2)^2}; \qquad B_{2l} = -\sqrt{\frac{2}{\pi}}\frac{Pht_l^{5/2}}{\pi\mu(t_l^2 + h^2)^2} \tag{80}$$

with $l = 1, 2, \ldots, N$; the unknowns $\mathbf{\Lambda}_{2l-1}$ and $\mathbf{\Lambda}_{2l}$ correspond to $\Phi(t_l)$ and $\Psi(t_l)$, respectively.

The stress intensity factors at the boundary of the penny-shaped crack can be obtained from the results

$$\mathrm{K}_{\mathrm{I}}^a = -\frac{\mu}{\sqrt{a}}\Lambda_{2N-1}; \quad \mathrm{K}_{\mathrm{II}}^a = -\frac{\mu}{\sqrt{a}}\sqrt{\frac{2}{\pi}}\Lambda_{2N}. \tag{81}$$

4 Numerical results and discussion

The analytical results and the computational approach presented in the paper can be used to evaluate the *displacement* and *stress fields* in the layer and halfspace regions, even though it entails tedious numerical evaluations of integrals involving fractional order Bessel functions, and the numerical solutions of the sets of integral equations defined by (41) and (78). A better use of the analytical approach is to develop results that will be of interest to *fracture mechanics* of the penny-shaped crack during the application of the Boussinesq force. In particular, these relate to the stress intensity factors that can arise due to the interaction between the penny-shaped crack and the Boussinesq force. The development of the stress intensity factors follows a distinct pattern depending on the sense of application of the Boussinesq force. When the Boussinesq force induces smooth closure of the entire penny-shaped crack, the Mode I stress intensity factor is suppressed. The variation of the Mode II stress intensity factor with the position of the penny-shaped crack is shown in Fig. 6. As is evident, the Mode II stress intensity factor reaches a maximum at a specific value of h/a and, since both $f(r)$ and $g(r)$ are *independent* of the elastic properties of the halfspace, the position of the peak value of K_{II}^{a} occurs at a fixed location for any isotropic elastic material, at$(h/a) \simeq 0.75$. The self-similar Mode II crack extension is attained when $\mathrm{K}_{\mathrm{II}}^{a} = \mathrm{K}_{\mathrm{II}}^{C}$, where $\mathrm{K}_{\mathrm{II}}^{C}$ is the Mode II critical stress intensity factor. It should, however, be noted that this mode of crack extension could be influenced by the development of separation at the closed crack surface, in which case the correct analysis of the problem will require the solution of the mixed boundary value problems shown in Fig. 4 that also can involve advancing and receding contacts.

For Boussinesq loads directed away from the surface of the halfspace, both Mode I and Mode II stress intensity factors are present. Figure 7 illustrates the variation of the normalized stress intensity factors as a function of the normalized depth of location of the penny-shaped crack. Again, since both $f(r)$ and $g(r)$ are independent of the elastic properties of the halfspace, the stress intensity factors developed are applicable to *any isotropic linear elastic solid*. The analysis indicates that $\mathrm{K}_{\mathrm{II}}^{a} > \mathrm{K}_{\mathrm{I}}^{a}$, implying that self-similar crack extension is possible if $\mathrm{K}_{\mathrm{I}}^{C} >> \mathrm{K}_{\mathrm{II}}^{C}$. In general, this property is satisfied by most brittle elastic materials. Alternatively, mixed mode fracture processes could arise, leading to crack extension in a crack deviation mode similar to the processes observed in the classic studies by Obreimoff [40] and in modelling indentation-induced mixed-mode crack extension [41]. Additional computations indicate that, regardless of the sense of application of the Boussinesq forces, if the penny-shaped crack is located at a relative depth $(h/a) > 5$, the surface loading has little influence on the development of conditions necessary for crack extension.

Acknowledgements The work described in this paper was supported by a Discovery Grant awarded by the Natural Sciences and Engineering Research Council of Canada and the *James McGill Research Chairs* program. The constructive comments of the reviewers are duly acknowledged. The author is grateful to a former research associate Dr. M.C. Au for assistance with the numerical work.

References

1. Boussinesq J (1885) Applications des potentials à l'étude de l'équilibre et du mouvement des solides élastique. Gauthier-Villars, Paris
2. Davis RO, Selvadurai APS (1996) Elasticity and geomechanics. Cambridge University Press, Cambridge
3. Selvadurai APS (2007) The analytical method in geomechanics. Appl Mech Rev 60:87–106
4. Selvadurai APS (2000) Partial differential equations in mechanics, vol 2. The biharmonic equation, Poisson's equation. Springer, Berlin
5. Selvadurai APS (2001) On Boussinesq's problem. Int J Eng Sci 39:317–322
6. Mindlin RD (1936) Force at a point in the interior of a semi-infinite solid. Physics 7:195–202
7. Lord Kelvin (1848) Note on the integrations of the equations of equilibrium of an elastic solid. Camb Dublin Math J 3:87–89
8. Love AE (1927) A treatise on the mathematical theory of elasticity. Cambridge University Press, Cambridge
9. Westergaard HM (1952) Elasticity and plasticity. Harvard University Press, Cambridge
10. Fröhlich OK (1934) Druckverteilung im baugrunde. Mit besonderer berücksichtigung der plastischen erscheinungen. Julius Springer, Wien
11. Selvadurai APS (2014) On Fröhlich's solution for Boussinesq's problem. Int J Numer Analyt Meth Geomech 38:925–934
12. Cotterell B (2010) Fracture and life. Imperial College Press, London
13. Sneddon IN (1946) The distribution of stress in the neighbourhood of a crack in an elastic solid. Proc R Soc Ser A A228:229–260
14. Sack RA (1946) Extension of Griffith's theory of rupture to three dimensions. Proc Phys Soc 58:729–736
15. Sneddon IN (1972) The use of integral transforms. McGraw Hill, New York
16. Sneddon IN (ed) (1977) Application of integral transforms in the theory of elasticity. International Centre for Mechanical Sciences, Courses and Lectures No. 220, Springer, Vienna
17. Hunter SC, Gamblen D (1974) The theory of a rigid circular disc ground anchor buried in an elastic soil either with or without adhesion. J Mech Phys Solids 22:371–399

18. Selvadurai APS (1980) Asymmetric displacements of a ground anchor embedded in a transversely isotropic elastic medium of infinite extent. Int J Eng Sci 18:979–986
19. Keer LM (1975) Mixed boundary value problems for a penny-shaped cut. J Elast 5:89–98
20. Selvadurai APS (1993) The axial loading of a rigid circular anchor plate embedded in an elastic halfspace. Int J Numer Anal Meth Geomech 17:43–353
21. Selvadurai APS (1994) On the problem of a detached anchor plate embedded in a crack. Int J Solids Struct 31:1279–1290
22. Selvadurai APS (2002) Mechanics of a rigid circular disc bonded to a cracked elastic halfspace. Int J Solids Struct 39:6035–6053
23. Smith FW, Alavi MJ (1971) Stress intensity factors for a penny-shaped crack in a halfspace. Eng Fract Mech 3:241–254
24. Srivastava KN, Singh K (1969) The effect of a penny-shaped crack on the distribution of stress in a semi-infinite solid. Int J Eng Sci 7:469–490
25. Erdogan F, Arin K (1971) Penny-shaped crack in an elastic layer bonded to dissimilar halfspaces. Int J Eng Sci 9:213–232
26. Sneddon IN, Lowengrub M (1969) Crack problems in the classical theory of elasticity. Wiley, New York
27. Kassir MK, Sih GC (1975) Mechanics of fracture three-dimensional crack problems, vol 2. Noordhoff International, Leyden
28. Cherepanov GP (1979) Mechanics of brittle fracture (Translation Editors R. de Witt and W.C. Cooley). McGraw-Hill, New York
29. Broberg KB (1999) Cracks and fracture. Academic Press, San Diego
30. Green AE, Zerna W (1968) Theoretical elasticity. Oxford University Press, Oxford
31. Little RW (1973) Elasticity. Prentice-Hall, Upper Saddle River
32. Barber JR (2002) Elasticity. Kluwer Academic Publishers, Dordrecht
33. Podio-Guidugli P (2014) Elasticity for geotechnicians: a modern exposition of Kelvin, Boussinesq, Flamant, Cerruti, Melan and Mindlin problems. Solid mechanics and its applications, vol 204. Springer, Switzerland
34. Baker CTH (1977) The numerical treatment of integral equations. Clarendon Press, Oxford
35. Delves LM, Mohamed JL (1985) Computational methods for integral equations. Cambridge University Press, Cambridge
36. Atkinson KE (1997) The numerical solution of integral equations of the second kind. Cambridge University Press, Cambridge
37. Selvadurai APS (2000) An inclusion at a bi-material elastic interface. J Eng Math 37:155–170
38. Selvadurai APS (2003) On the loading of an annular crack by a disc inclusion. J Eng Math 46:377–393
39. Copson ET (1961) On certain dual integral equations. Proc Glasgow Math Assoc 5:21–24
40. Obreimoff JW (1930) The splitting strength of mica. Proc R Soc A217:290–297
41. Selvadurai APS (2000) Fracture evolution during indentation of a brittle elastic solid. Mech Cohesive-Frict Mater 5:325–339